Max-Planck-Institut
für Meteorologie

# REPORT No. 154

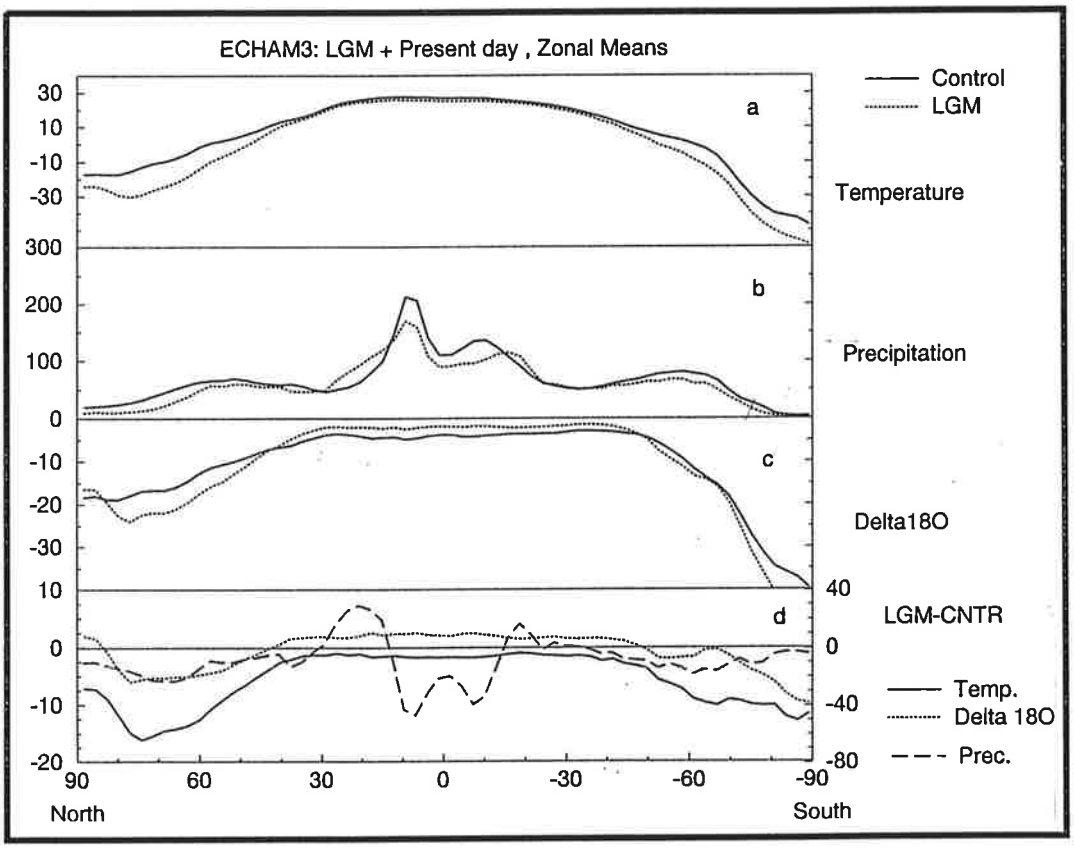


# WATER ISOTOPE MODELING IN THE ASIAN MONSOON REGION

by

GEORG HOFFMANN · MARTIN HEIMANN

HAMBURG, September 1994

AUTHORS:

Georg Hoffmann
Martin Heimann

Max-Planck-Institut
für Meteorologie

MAX-PLANCK-INSTITUT
FÜR METEOROLOGIE
BUNDESSTRASSE 55
D-20146 Hamburg
F.R. GERMANY

Tel.: +49-(0)40-4 11 73-0
Telefax: +49-(0)40-4 11 73-298
E-Mail: <name> @ dkrz.d400.de

# Water Isotope Modeling In The Asian Monsoon Region

Georg Hoffmann
Martin Heimann
Max-Planck-Institut
für Meteorologie

February 1, 1995

**Abstract**

The isotopic composition of paleoprecipitation is widely used as a proxy data for temperature and precipitation. In order to investigate the validity of these transfer functions for water isotopes, oxygen 18 and deuterium, we installed a water isotope model into the ECHAM Atmospheric General Circulation Model (AGCM). Such an isotope model calculates all fractionations between the stable water isotopes in the hydrological cycle of the AGCM. We ran the model under present day conditions and under the boundary conditions of the Last Glacial Maximum (LGM) for four years each.

On a global scale the model satisfactorily reproduces the main features of the water isotopes in the hydrological cycle (temperature effect, amount effect). The analysis focusses on the Asian monsoon area where atmospheric circulation strongly affects the seasonal cycle of water isotopes in precipitation. The model successfully simulates the influence of circulation, temperature and precipitation amount in this region under present day conditions.

Under LGM conditions the model shows a weakened summer monsoon causing a strong positive isotope signal over East Asia although the continent is about 2-4°C cooler than today. This result underlines the difficulties to use the isotopic composition of paleoprecipitation simply as a measure of temperature. Furthermore, it demonstrates the importance of circulation changes and of changing moisture sources for the interpretation of a given isotope signal.

ISSN 0937-1060

# 1 Introduction

Since the landmark paper of Dansgaard 1964 (Dansgaard 1964), the use of the stable water isotopes $^1H_2\,^{18}O$and $^1H^2H\,^{16}O$has been established in paleoclimatology studies. These isotopes are heavier and less diffusive than "normal" water $^1H_2\,^{16}O$and therefore undergo fractionation processes during any phase transition. Within the global water cycle the liquid or solid phase is enriched in heavier isotopes and the vapour phase correspondingly depleted. The degree of enrichment (depletion) is described by the fractionation coefficient $\alpha$. The temperature dependence of $\alpha$ has been measured very exactly in the laboratory (Majoube 1971): A colder temperature during a phase transition leads to a stronger isotope fractionation. The isotopic composition of water is usually expressed as deviations in permill from the Vienna standard $R_{SMOW}$ [1] (SMOW=Standard Mean Ocean Water):

$$\delta = \frac{R_{Sample}}{R_{SMOW}} - 1 \tag{1}$$

Discussing the isotope data of rain and snow sampled by the recently established network of the International Atomic Energy Agency (I.A.E.A.) Dansgaard demonstrated the usefulness of $^{18}O$ and $^2H$ (deuterium) as a proxy data for temperature and precipitation. Basically two effects influence the isotopic composition of precipitation: the temperature effect and the amount effect.

In the temperature range below 15°C there exists a linear relationship between the $\delta$ value of precipitation and the surface temperature at the precipitation site. This temperature effect may be interpreted by means of a simple two–phase condensation model. Vapour with a prescribed temperature dependent isotopic composition is brought to isothermal or isobaric condensation. Under the assumption of an open ("Rayleigh") system the condensate is removed immediately after formation without any further isotopic exchange with vapour. During the condensation process the vapour and subsequently the liquid gets more and more depleted. The model portrays the global water cycle in simplified terms: evaporation at warm temperatures in the tropics and subtropics, transport to high latitudes and condensation. The $\delta$ value of precipitation $\delta_P$ is proportional to the degree of rainout, i.e. $\delta_P \sim f^{\bar{\alpha}-1}$ with $f = \frac{q(t)}{q_{ini}}$ (2), q(t) as the current mixing ratio of water vapour, $q_{ini}$ as the mixing ratio at the evaporation site and $\bar{\alpha}$ as a mean fractionation coefficient. It is worth to mention that the strength of the rainout f and not the temperature dependence of the fractionation coefficient is the leading mechanism responsible for the temperature effect.

The second important effect analyzed by Dansgaard in the I.A.E.A. data is the amount effect i.e., a linear relationship between the amount of precipitation and the $\delta$ value observed mainly in convectively very active regions. In particular the precipitation captured on tropical islands or at monsoon related stations shows a strongly depleted isotope signal in the rainy season and an only slightly depleted signal in the dry season. Dansgaard proposed three mechanisms to explain the amount effect. The first argument again is based on the "Rayleigh model". A vapour

[1] The $\frac{^{18}O}{^{16}O}$ isotope concentration of SMOW is $R_{SMOW} = 2005.20 * 10^{-6}$

mass lifted up within a strong convective event rains out almost completely (small f in (2)). The rain formed from such a vapour mass is only slightly fractionated at the beginning of a convective shower and gets lighter at the end when the rainout process finishes. The only difference to the temperature effect is that the air mass is moved vertically instead of being transported horizontally to high latitudes. The strength of the convective activity may be influenced by the position of the InterTropical Convergence Zone (ITCZ) or is orographically forced but is nearly independent of the surface temperature. Indeed, the $\delta$ - temperature relation breaks down above 15°C, where the $\delta$ - precipitation relation dominates. An additional second and third process concern raindrops below the cloud base. The isotopic exchange of falling drops with surrounding vapour and the evaporative enrichment of such drops is most pronounced for light rains and strongly reduced for heavy showers. Both mechanisms amplify the amount effect.

Fortunately, the isotopic composition of paleoprecipitation can be deduced from a variety of recorders like the shells of land snails (Goodfriend 1991) and of fresh water molluscs (Covich and Stuiver 1974), the inorganic carbonate sediments of fresh water lakes (Stuiver 1970, Eicher and Siegenthaler 1976, Gasse et al. 1991), paleowaters (Sonntag et al. 1978), fluid inclusions in speleothems (Harmon and Schwarz 1981, Harmon et al. 1981), the tree ring cellulose of ancient trees (Yapp and Epstein 1977, Lipp et al. 1991, Becker et al. 1991), tropical corals (Cole and Fairbanks 1990, Fairbanks and Matthews 1978) and ice cores of glaciers (Grootes et al. 1989, Thompson et al. 1989) and of the large Greenlandian (Johnsen et al. 1992) and Antarctic (Lorius et al. 1985) ice sheets. These proxy data are covering different episodes of earth history and have different time resolution up to annual layers, e.g. corals and ice cores.

But, although the explanation for the two dominating effects, temperature and amount effect, is widely accepted, the interpretation of a reconstructed $\delta$ - value of paleoprecipitation in terms of temperature- or precipitation changes is still under debate. Fundamentally different climate conditions possibly prevailing during the Last Glacial Maximum (LGM) could create completely different pathways of moisture masses from their formation to their precipitation site. Thereby these air masses experience a different rainout history which ends in a different isotope signal in precipitation. These variations are not completely explained by local temperature or precipitation changes. The scatter in the present day $\delta$ -temperature relation (Fig.3b) is about 10% of the entire variability and is mainly caused by the variability of atmospheric circulation. (Cole et al. 1993) point out that this scatter partly exceeds the observed change of the $\delta$ value between holocene and LGM. In order to obtain insight into the structure and the importance of such circulation changes for the isotope signal a new approach to this problem has recently been undertaken by incorporating the water isotopes in General Circulation Models (GCM's) (Joussaume et al. 1984, Jouzel et al. 1987, Hoffmann and Heimann 1993). These threedimensional models take into account the mixing of air masses and changes in moisture pathways as mentioned above, the conditions at the evaporation site (temperature,moisture) and at the condensation site (cloud internal temperatures, liquid cloud water) as well. Also, the reevaporation and the isotopic exchange of rain droplets with surrounding vapour, which could not be considered in simple Rayleigh

models, is included in the isotope part of a GCM's water cycle.

We present here the results of our water isotope model which is embedded into the ECHAM3 GCM, the climate model developed at the Max-Planck-Institut für Meteorologie. We ran the model under present day and LGM boundary conditions as prescribed by the Paleo Modelling Intercomparison Project (PMIP) (WMO 1993). Our analysis focusses on the Asian monsoon regions: India, Southeastern Asia and China. Here, the strong seasonal circulation changes from the rainy summer monsoon to the dry winter monsoon and the complex spatial distribution of temperature dominated and precipitation amount dominated isotope signals represents a real challenge to water isotope models. Further, previous studies with GCM's have shown that the monsoon circulation is strongly affected by changing paleoclimatic boundary conditions (Kutzbach and Guetter 1986, Prell and Kutzbach 1987, Rind 1987). A colder Asian continent during the LGM reduces the temperature gradient from land to the Indian ocean in summer and amplifies this gradient in winter. This weakens the southwestern summer monsoon and intensifies the northeastern winter monsoon. We try to clarify the consequences for the isotopic signals resulting from such a paleo scenario.

In Chapter 1 we briefly introduce our water isotope model. For more details see (Hoffmann 1995). In Chapter 2 we describe the performed numerical experiments. Chapter 3 contains the assessment of simulated isotope results by comparing the annual mean and the seasonal cycle with observations of the I.A.E.A.. The changes in the atmospheric circulation in the Asian monsoon region under LGM conditions and their consequences for the water isotopes are described in Chapter 4.

# The Model

The ECHAM3 model is the Cycle 3 version of the atmospheric GCM at the Max-Planck-Institut für Meteorologie in Hamburg. It is based on the weather forecast model of the European Center for Medium-Range Weather Forecasts (ECMWF). The resolution of the spectral model used in these experiments is the T42 resolution which corresponds on the physical grid to a 2.8 ° * 2.8 ° resolution. The transport of moisture, liquid cloud water and their corresponding isotope fields is calculated by a semi-Lagrangian transport scheme. There are two types of clouds simulated in the model: Large scale clouds and convective clouds. Large scale clouds form typically during gentle ascent in extratropical cyclones and have an extent of several hundred kilometers, whereas convective clouds develop mainly in the tropics from nearly vertical ascent caused by moist adiabatic instability. Their extent is several kilometers. The model takes into account a subgrid scale cloud cover in every grid box and allows the calculation of cloud internal quantities like temperature and humidity, which differ from the cloud free part. Convective clouds are described by a massflux scheme. For a more complete description of the GCM see (Modellbetreuungsgruppe 1992).

Fig.1 shows the most important processes within the global water isotope cycle. The first fractionation in the cycle takes place during the evaporation from the ocean and depends upon relative humidity, wind velocity and temperature. The

ocean is assumed to be isotopically uniform ($R_{SMOW}$) with a slight evaporative enrichment in the upper most layer (about 0.5‰ for $^1H_2\,^{18}O$). The description of the non-equilibrium (kinetic) effects at the ocean surface determining the global relation of oxygen 18 and deuterium is taken from (Merlivat and Jouzel 1979). Condensation in clouds is treated in two different ways: as an open system or as a closed system (Dansgaard 1964). Snow forms isotopically in an open system, which assumes isotopic equlibrium only between the fraction of snow just formed and the surrounding vapour. Afterwards this fraction is removed directly from the system and does not interact further with the vapour. This is justified by the extrem low diffusity of water isotopes in snow and ice. Condensation of droplets is treated as a closed system i.e., within one timestep the formed droplets are in isotopic equilibrium with the vapour in the cloud. The non- equilibrium effect during the sublimation of snow caused by the oversaturation in the vicinity of ice crystals has been adapted from (Jouzel and Merlivat 1984, Jouzel et al. 1987). Also, reevaporation of falling droplets below the cloud base and isotopic exchange of these droplets, which both result in an enrichment of rain, have been considered according to (Stewart 1975). The surface scheme of ECHAM comprises three different water reservoirs: a thin skin layer which corresponds to water remaining at the surface after a shower, the surface soil wetness and the snow. It has been shown that evapotranspiration of plants at least in the steady state does not fractionate water isotopes: the groundwater signal is preserved during its flux through the stem and the stomata to the air

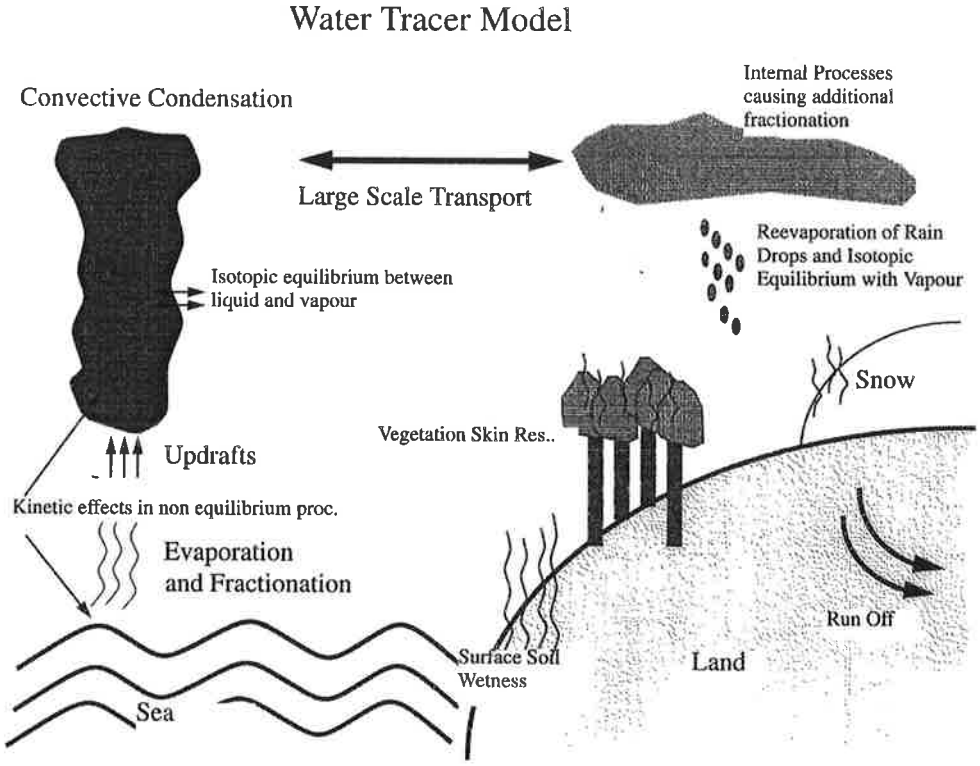


Figure 1: Scheme of the water isotope cycle in the ECHAM model.

(Zimmerman et al. 1967, White 1989). Because evapotranspiration is the dominating evaporative flux from land nearly all over the world no fractionation is included in the evaporation from the three surface water reservoirs. The calculation of surface runoff of the isotopes parallel to "normal" water closes the isotopic water cycle.

# 2 The Experiments

The control run was started in the 18'th month of a previous control run simulation and is subsequently integrated over $5\frac{1}{2}$ years. We used climatological Sea Surface Temperatures (SST) as lower boundary condition. The atmosphere was initialized with a uniform $\delta$ value in vapour and in cloud liquid water (for $^{18}O$ : $\delta_{vap} and \delta_{clw} = -80$ ‰). The surface water reservoirs were initialized according to the observed global $\delta$ - temperature relation ( $\delta\,^{18}O = 0.69$ ‰T -13 ‰). After about 2-3 months the system has already reached isotopic equilibrium. The results presented here are based on the last 5 years of the control run.

For the LGM simulation, we took the sea surface temperatures reconstructed by the CLIMAP group (CLIMAP:81 1981) as lower boundary condition and the only slight insolation changes calculated by Berger (Berger 1978) as upper boundary condition. Informations about the glacial/interglacial shift in coastlines due to the sealevel decrease of about 120m and the new ice sheet reconstruction was taken from (Tushingham and Peltier 1991). We ran the model for $5\frac{1}{2}$ years and initialized the water isotopes after the first year similarly to the control run. Because the ice sheets consisted of isotopically strongly depleted water the remaining ocean was prescribed about 1.6 ‰ (Duplessy et al. 1980) in $^{18}O$ heavier than today. We analyzed the last four years of the paleo simulation.

# 3 The Water Isotope Cycle Under Present Day Conditions

## 3.1 Global Behaviour

Fig.2 shows the 5 years mean of the control run of the $\delta\,^{18}O$ value of precipitation. The monthly means of $\delta\,^{18}O$ were weighted with the monthly amount of precipitation and subsequently averaged. This tends to lower the $\delta$ -values compared to the unweighted values due to the amount effect mainly in the tropics and subtropics (Dansgaard 1964). Instead of comparing this result pointwise with the measurements of the I.A.E.A. we describe only some general features of the simulation before focussing on the monsoon regions. The isotopic composition of precipitation over the oceans between roughly 40 °N and 40°S varies only slightly from -4‰ up to -1‰. The rainout is still weak here and the isotopic composition of vapour over the ocean surface is almost constant (between -11. and -12. ‰) preventing also a large variability of the $\delta$ values of precipitation. Polewards the latitudinal structure of the $\delta\,^{18}O$ values is produced by stronger rainout of air masses at lower temperatures. The

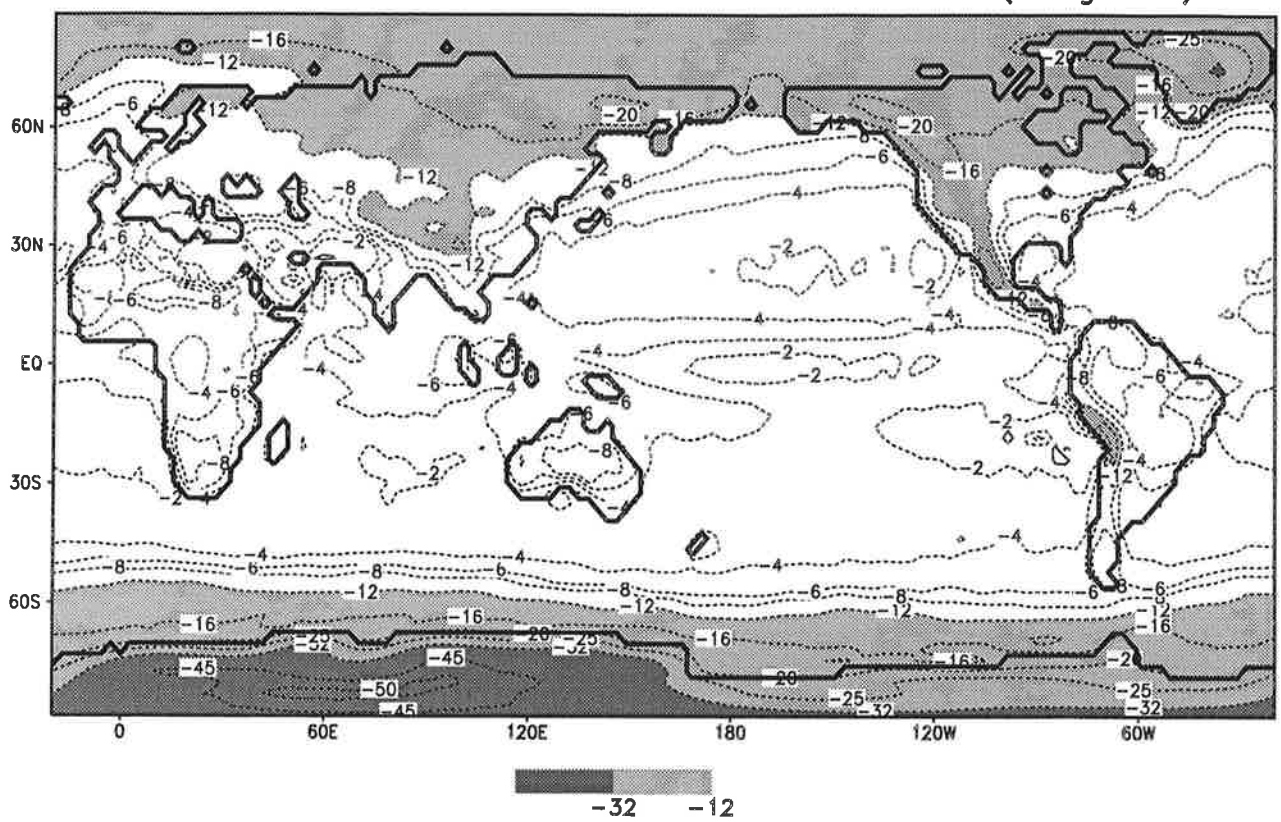


Figure 2: Mean of $\delta^{18}O$ over 5 years of the control run. The monthly $\delta^{18}O$ are weighted with the monthly precipitation.

most depleted precipitation in the northern hemisphere can be found over the top of the Greenland ice sheet: the model result of -33.2 ‰ is in fairly good agreement with the observed -34.8 ‰ (Johnsen et al. 1992). The rainout in the Antarctic is more complete due to lower temperatures and the larger distance of the top of the East Antarctic ice sheet from oceanic vapour sources. The most negative $\delta$ value in the model (63E,83S) is about 4 ‰ too weak fractionated compared with the most negative values observed in Vostok (-57‰) (Lorius 1983). This difference may again be partly due to the model orography. The importance of the orography for the rainout process can also be inferred from the isotope patterns along the large mountain chains: the Himalayas, the Andes and the Rocky Mountains. At these orographic obstacles air masses are lifted up and subsequently rain out strongly ("altitude effect" (Dansgaard 1964)).

Further, the isotopic composition of precipitation measures the "continentality" of vapour masses which are transported from sea to land by the general circulation. Again the degree of rainout is responsible for the isotopic gradient from the coast to the interior of a continent simulated by the model: 1) From the gulf of Mexico northwestward into North America. 2) From England with the westerlies into Europe. 3) From the tropical Atlantic with the trade winds into the Amazon basin. 4) From the Chinese Sea with the monsoon circulation into China. Over Europe and the Amazone basin, where the data of the I.A.E.A. allow a comparison with the observation, the model seems to simulate quite satisfactorily this "continental effect": The simulated gradient over Europe is approximately -.3 ‰ per 100km eastward

(observerd 0.33‰ per 100km (Rozanski et al. 1982) ) and in the Amazone basin the gradient is -0.08 ‰ per 100 km westward (observed -.075‰ per 100 km (Salati et al. 1979)). The reduced gradient over South America is due to the higher degree of recycling of precipitation.

The strongest precipitation in the tropics can be found along the Intertropical Convergence Zone (ITCZ). Because of the amount effect we can recognize clearly this area charaterized by strong convective activity and heavy showers over the West Pacific warm pool and two asymmetric branches north and south of the equator. The isotope values here vary between -4 ‰ and -7‰ which is in accordance with the observations (IAEA 1992).

The model has problems to simulate a realistic isotopic composition in some dry

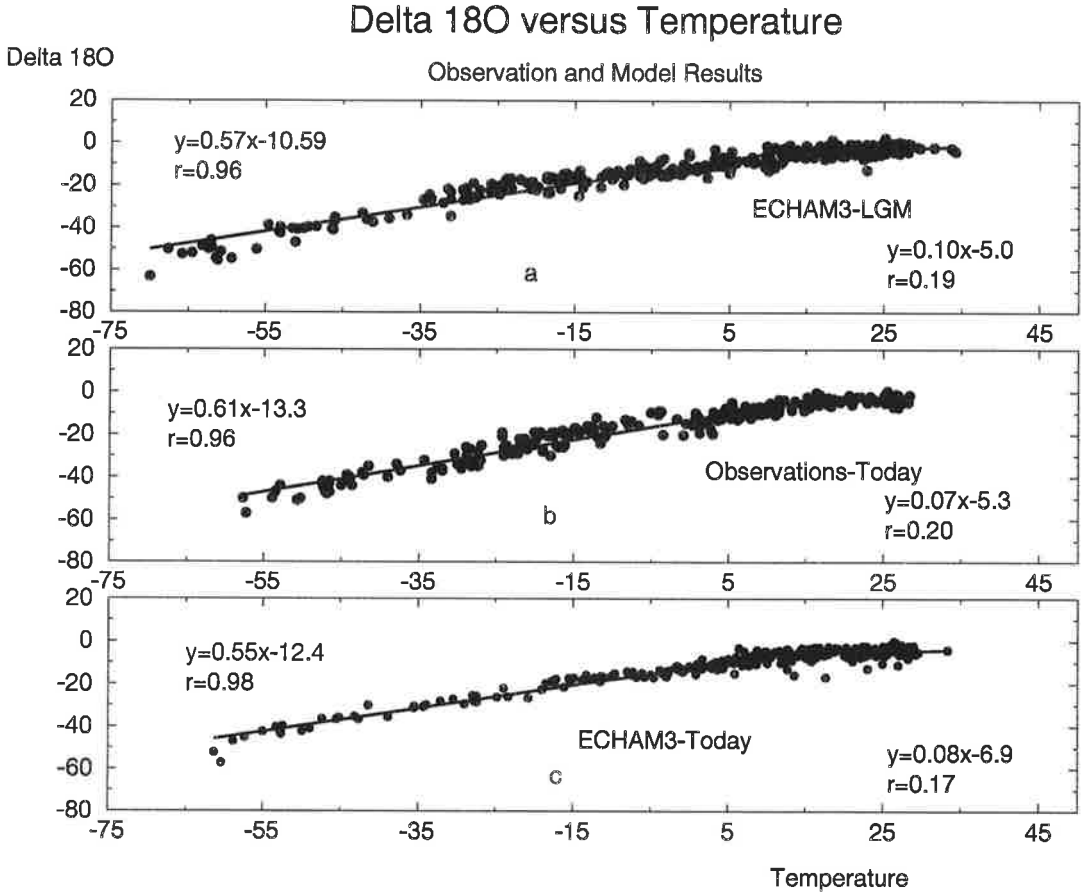


Figure 3: Annual mean of $\delta^{18}O$ versus annual mean of surface temperature from observations (b) and the model integrations: under present day conditions (c) and under LGM conditions (a). The observations contain all IAEA stations (IAEA 1992) wich have been measured continuously for at least one year. $\delta^{18}O$ measurements of firn from Greenland and Antarctic have been added. They have been gratefully provided by R.Koster and J.Jouzel and are cited in (Jouzel et al. 1987). We have plotted the results of the model gridpoints, which correspond to the observation sites. The linear regressions are calculated in two temperature ranges:below and above 15°C.

The model has problems to simulate a realistic isotopic composition in some dry areas like the west and central Sahara, the Ethiopian highland and the interior of Australia. Although there are almost no stations of the I.A.E.A. in these regions the computed $\delta$ values between -6 ‰ and -9‰ are certainly much too low. The reason for the strong fractionation under conditions of rare precipitation in the model is not yet understood.

The capacity of the model to simulate the temperature effect globally is given in Fig.3b+c where the relation between the annual mean temperature and $\delta^{18}O$ of precipitation in the observations and in the ECHAM model are shown. The correlation between T and $\delta^{18}O$ of precipitation in the lower temperature range is similarly high in both cases (r=0.96 in the observations and r=0.98 in the model), but the slope of the regression line is about 10% too flat in the model. Because a previous run with a coarser resolution showed still a less steep relation between T and $\delta^{18}O$ this deficiency may at least partly be due to the orographic resolution of the model. Above 15°C there is no correlation in the model between T and $\delta^{18}O$ (r=0.17 in the model, r=0.2 in the observations).

## 3.2 The Water Isotopes In The Monsoon Area

Fig.4 shows the monthly and annual mean of precipitation and $\delta^{18}O$ for two groups of stations: tropical islands and stations in the Asian monsoon regions. The isotope signal measured on tropical islands should represent examples clearly dominated by the amount effect. The vapour source is isotopically very uniform. Therefore, the wind direction should not be important and mainly the strength of the convective activity controlles the isotopic composition of rain. In the tropics, the correlation of $\delta^{18}O$ to the amount of precipitation is quite high in the observations (r=-.91 for the monthly means) and in the model (r=-.82). However, the slope of this relation is about 80% too flat in the model (about 1‰ $\delta^{18}O$ per 100mm compared with 1.8 ‰ per 100 mm in the observations). Different reasons could be responsible for this deficiency: Firstly, the simulation time of 5 years is rather short for a good statistical representation of the ITCZ in a GCM. Secondly, the numerical description of isotopic exchange of raindrops below the cloud base with the surrounding vapour is somewhat arbitrary. We have chosen a fraction of 45% of drops getting into equilibrium with vapour. The sensitivity of the amount effect in the model on this arbitrary chosen fraction has still to be tested. Thirdly, the underestimated slope could also indicate that the convection in the model does not reach high enough in altitude. The vapour in the upper troposphere is very depleted in the model (-40 – -50‰ in 5km, in accordance with observations (Taylor 1972)) and could influence significantly the isotopic composition of raindrops formed in convective towers.

The $\delta$ values at stations in the Asian monsoon region (Fig.4c+d) are much more affected by circulation changes than the stations on tropical islands. As there are two isotopically different vapour sources, the already depleted vapour over the continent and the vapour from the Indian ocean and the Pacific, the wind direction is more important for the isotopic composition of rain and hence the correlation of the $\delta$ values to the amount of precipitation is weaker (r=-.81 in the observation, r=-.76 in the model).

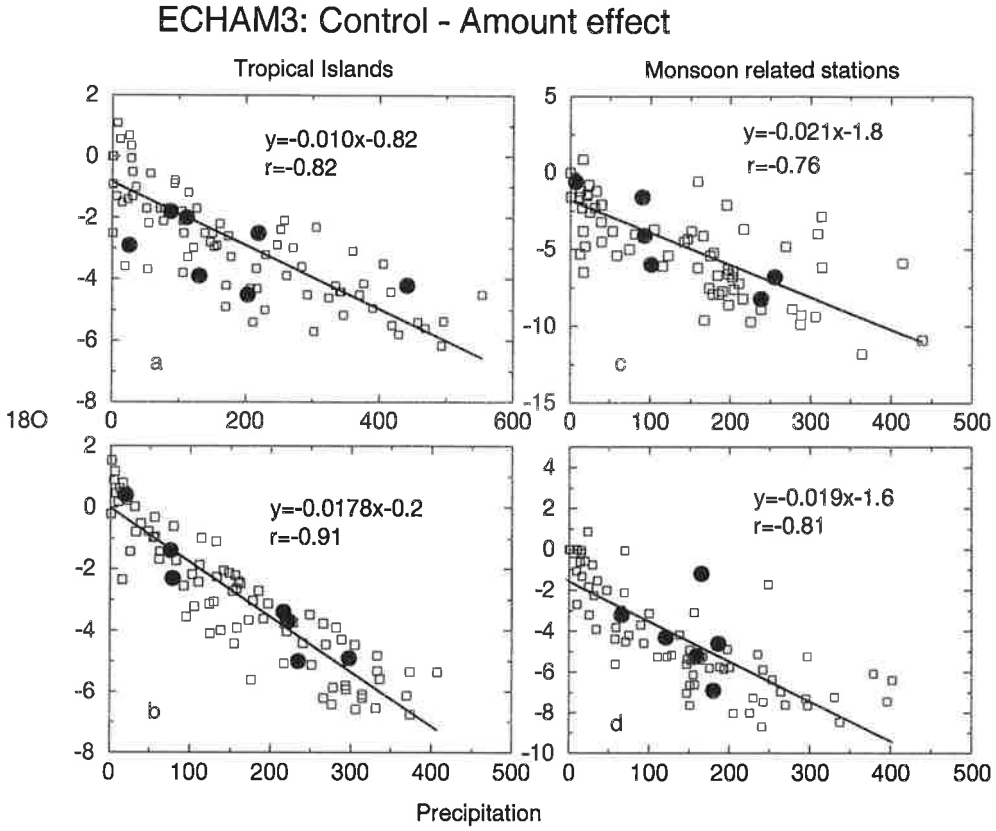


Figure 4: Annual means (filled dots) and monthly means (light squares) of $\delta^{18}O$ versus precipitation (mm/month) for tropical islands (b:observations from the IAEA stations Apia, Diego Garcia, Sao Tome, Taguac, Truk, Wake Isl. and Yap; a:corresponding model results of the control run) and for monsoon related stations (d:observations at Bombay, New Dehli, HongKong, Singapore, Bangkok and Djakarta; c: model results). The linear regressions are calculated for the monthly means.

This is also corroborated by the seasonal cycle of temperature, precipitation and $\delta^{18}O$ at two stations of the I.A.E.A. network, Bombay and HongKong (Fig.5a-f). A comparison of single stations with gridpoints of a GCM is problematic, because the orographic resolution in the model can not correctly take into account the sharp mountain chains which are very important for the simulation of the precipitation. Both coastal stations are located in front of such mountains which is why it is not surprising that the rain gauge is considerably underestimated by more than 200 mm per month during the summer monsoon. Because of too weak summer precipitation and the long dry period in winter the surface water reservoirs of the model tend to dry out. In particular at Bombay the lack of evaporative cooling causes too high temperatures in spring and early summer. Nevertheless, the seasonal cycle of $\delta^{18}O$ in HongKong seems to be reproduced quite well. The isotopic composition of rain is controlled by the amount effect (r=-.87 in the observations, r=-0.84 in the model). The minor role of the temperature for the rainout process above 15°C is demonstrated by the surprising inverse correlation of temperature and $\delta^{18}O$ (r=-.95 in the observations, r=-.75 in the model).

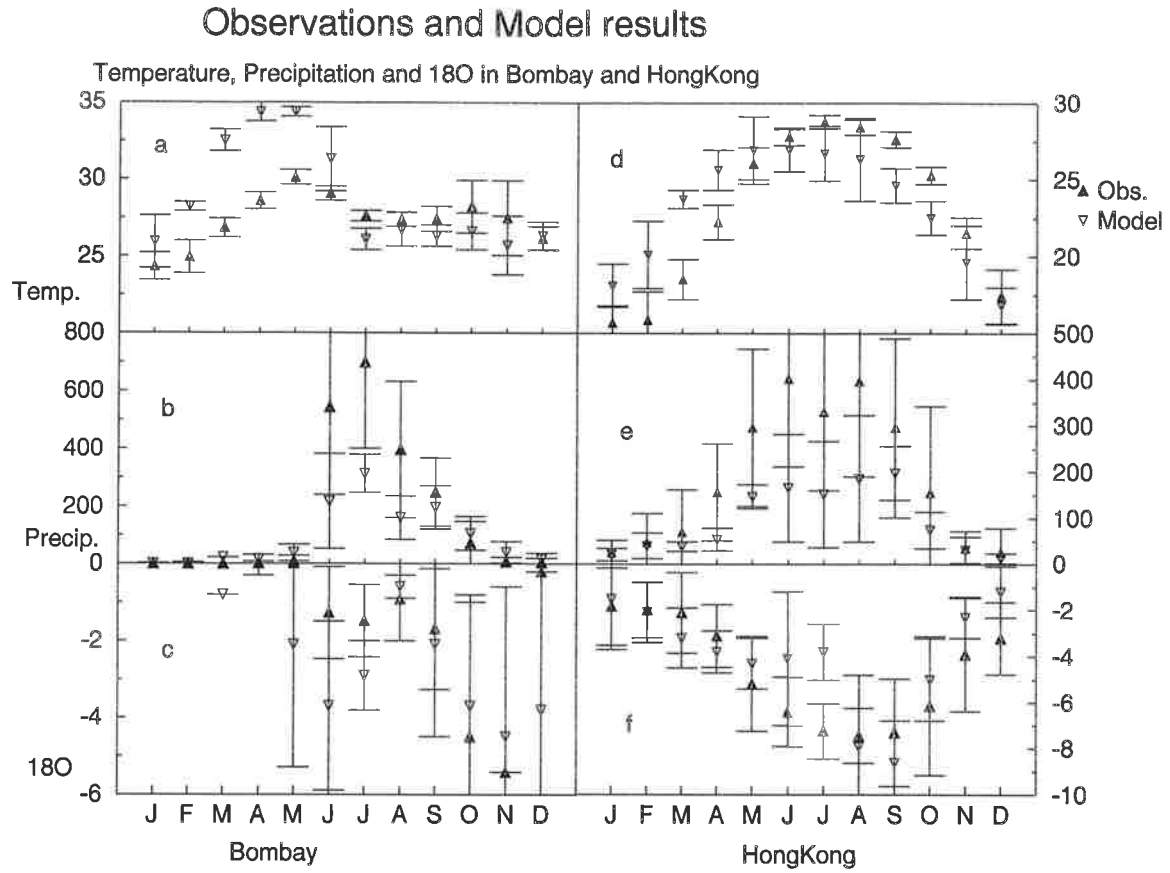


Figure 5: Fig.5a-f: Temperature (°C), precipitation (mm/month) and $\delta\,^{18}O$ for the IAEA stations Bombay (a-c) and HongKong (d-f). The filled triangles denote the observations, the light triangles denote the results of the corresponding model grid points.

circulation for the $\delta\,^{18}O$ value in this area. In the observation period of 11 years there was no precipitation during the first five months of the year. The abrupt onset of the monsoon fell always on June. During the main rain period from June to August the $\delta\,^{18}O$ values follow the amount effect. But with the end of the summer monsoon the winds turn slowly from the southwest to the northwestern winter monsoon transporting depleted vapour from the interior of India to Bombay. Although the precipitation amount is rather small from September to November the $\delta$ values indicate a more and more fractionated rain. This behaviour is captured quite satisfactorily by the model: From July to September the $\delta$ values follow the amount of precipitation, from October to December the precipitation is affected by the depleted vapour from the interior of India. Such continental and strongly fractionated vapour is probably also responsible for the deficient $\delta$ values in May and June which are about 2‰ too negative.

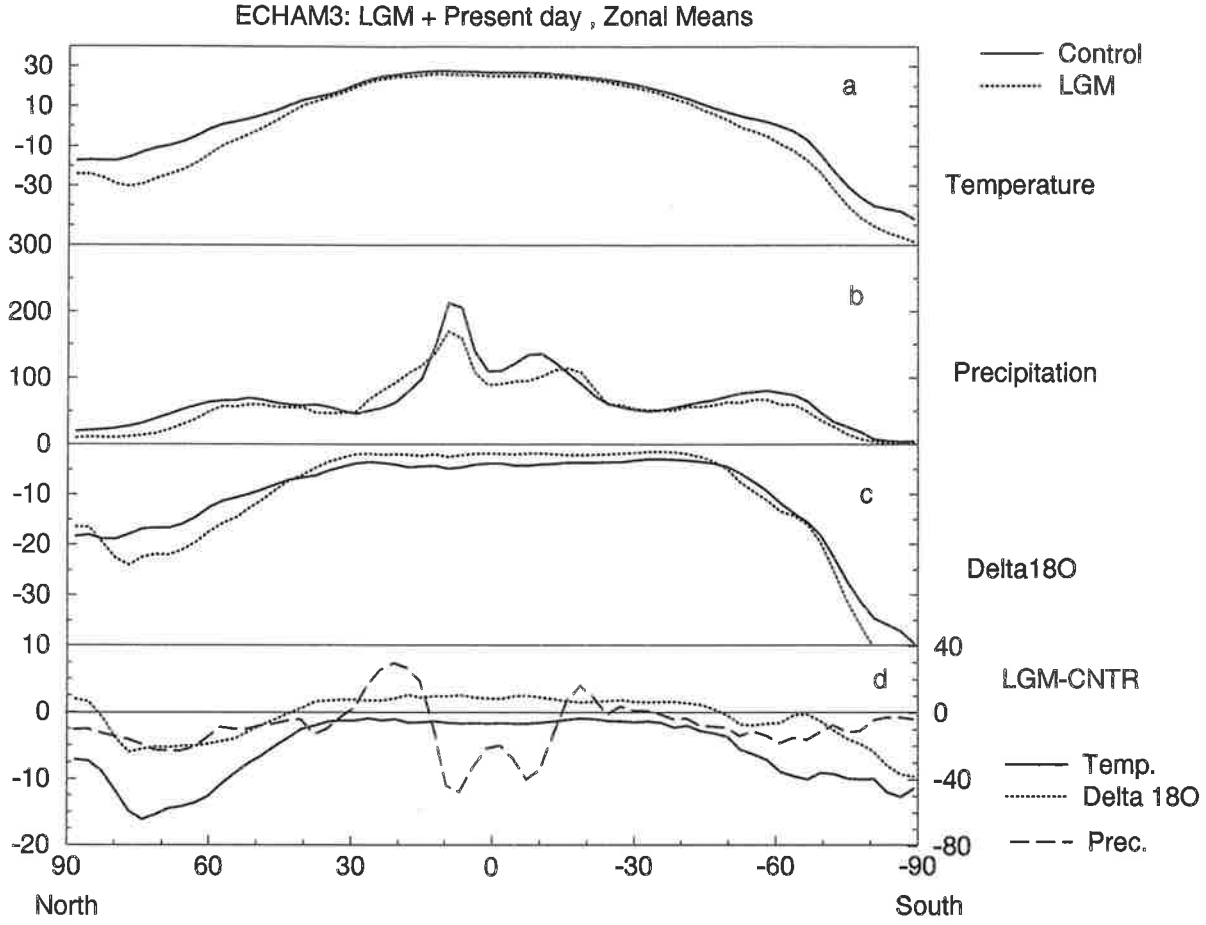


Figure 6: Zonal mean of (a) surface temperature (°C), (b) precipitation (mm/month) and (c) $\delta^{18}O$ for the simulations under present day conditions (solid lines) and under LGM conditions (stippled line). (d) shows the corresponding anomalies (LGM-today) for temperature, $\delta^{18}O$ (both left scale: °C and ‰) and precipitation (right scale: mm/month).

# 4 The LGM Run

## 4.1 Global Patterns

Focussing now on the modelled changes of the isotopic composition of rain under LGM conditions we attempt to determine to what extent measured changes in the $\delta^{18}O$ of paleoprecipitation are valuable recorders of temperature or precipitation changes in the monsoon region. (Fig.6a-c) show the zonal mean of temperature, precipitation and $\delta^{18}O$ under both boundary conditions. The simulated temperature changes (Fig.6a+d) are of course dominated by the prescribed CLIMAP sea surface temperatures. They are characterized by only slight and uniform temperature changes in the tropics and subtropics ($\sim$ 1-2°C) and stronger cooling in high latitudes. The strongest temperature signals are found in regions affected by the equatorward expansion of the polar front and over the icesheets. The model reacts on this temperature forcing with a global reduction of precipitation of about $10mm/m**2$ year. Compared to a previous simulation (Lautenschlager and Her-

terich 1990) with the older ECHAM2 in T21 resolution, the Hadley circulation in the tropics is much weaker in the present LGM simulation. Such tropical aridness is qualitatively confirmed by a variety of paleodata, e.g. by low lake levels in tropical Africa (Street-Perrot and Harrison 1985) and a suggested retreat of the tropical rainforest in the Amazon basin (Bradley 1985). Increases in precipitation in the subtropics are restricted to areas in the western Indian ocean and the Pacific, which are prescribed warmer than today in the CLIMAP reconstruction (Fig.7+8).

Clearly the zonal mean of $\delta^{18}O$ in precipitation (Fig.6c) under LGM conditions is not a simple linear shift of present day values. The latitudinal gradient of the $\delta^{18}O$ appears steeper than today. Simulated values are about 2-3 ‰ higher between 45°N and 45°S and up to 8‰ lower values in high latitudes. The reversal of this trend to positive anomalies in the Arctic seems to be unrealistic and is not yet clarified. The largest temperature anomalies are reached over the northern icesheets between 60°N and 80°N. North of 80°N there is a reversal of the temperature anomalies similar to the $\delta^{18}O$ anomalies. Nevertheless, the temperature anomaly is still negative in the Arctic actually producing a stronger rainout and more negative $\delta^{18}O$ values than today. A positive $\delta^{18}O$ anomaly would indicate a vapour source shifted far to the North compared with present day climate. Because of the greater sea ice extent and generally cooler temperatures in high latitudes such a local Arctic vapour source is highly unlikely under LGM conditions.

The simulated higher $\delta^{18}O$ values in the tropics could be explained by four different mechanisms: (1) the prescribed $\delta^{18}O$ level of the LGM ocean is 1.6‰ higher. (2) Cooler evaporation temperatures reduce the temperature gradient to the precipitation site. Therefore, the rainout process starts at a lower level ($q_{ini}$ smaller in 2) which results finally in a higher $\delta^{18}O$ value assuming that the condensation temperature remains the same. (3) Because of reduced precipitation in the tropics we expect higher $\delta^{18}O$ values due to the amount effect. (4) Because of the first three mechanisms less depleted vapour is transported to higher latitudes. This may be the reason why positive $\delta^{18}O$ anomalies extend farly over the region dominated by the amount effect nearly to mid-latitudes (45°N - 45°S).

## 4.2 The LGM Climate In The Monsoon Region

The Hadley circulation responds sensitively to the prescribed sea surface temperature changes based on CLIMAP in the Pacific and the Indian ocean. The approximately 2°C cooler tropical Pacific combined with the slightly warmer subtropical North and South Pacific disperse the tropical low pressure system considerably. This weakens the convergence of air in the ITCZ and hence the strength of the trade winds (Fig.7+8). The precipitation is diminished by about 100 to 200 mm per month. The areas with enhanced precipitation (about 30-100 mm) are the above mentioned regions with unchanged or even warmer SST's. Such precipitation anomalies following linearly the SST forcing has also been found in other GCM studies (Rind 1987, Kutzbach and Guetter 1986).

The summer monsoon (Fig.7) is weakened considerably under LGM conditions. There are surface wind anomalies against the monsoon circulation along the coast of Somalia and in the Arabian sea. Further, the surface wind anomalies over China

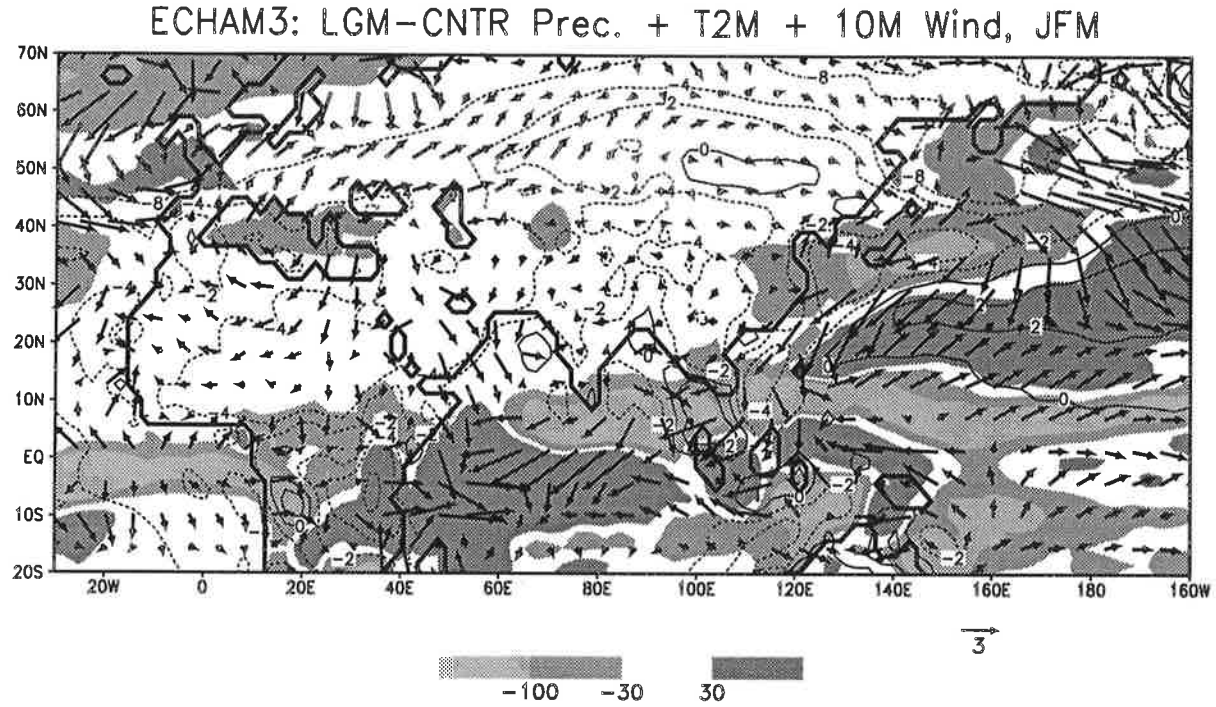


Figure 7: Simulated anomalies (LGM-today) of precipitation (mm/month; shading -100,-30,30 mm/month), 2 meter temperature (°C ; isolines are plotted at 2,0,-2,-4,-8 °C) and 10 meter wind (m/s ; the arrow below the plot denote an anomaly of 3m/s). The figure shows the results in the Asian monsoon area for the summer monsoon (July,August,September).

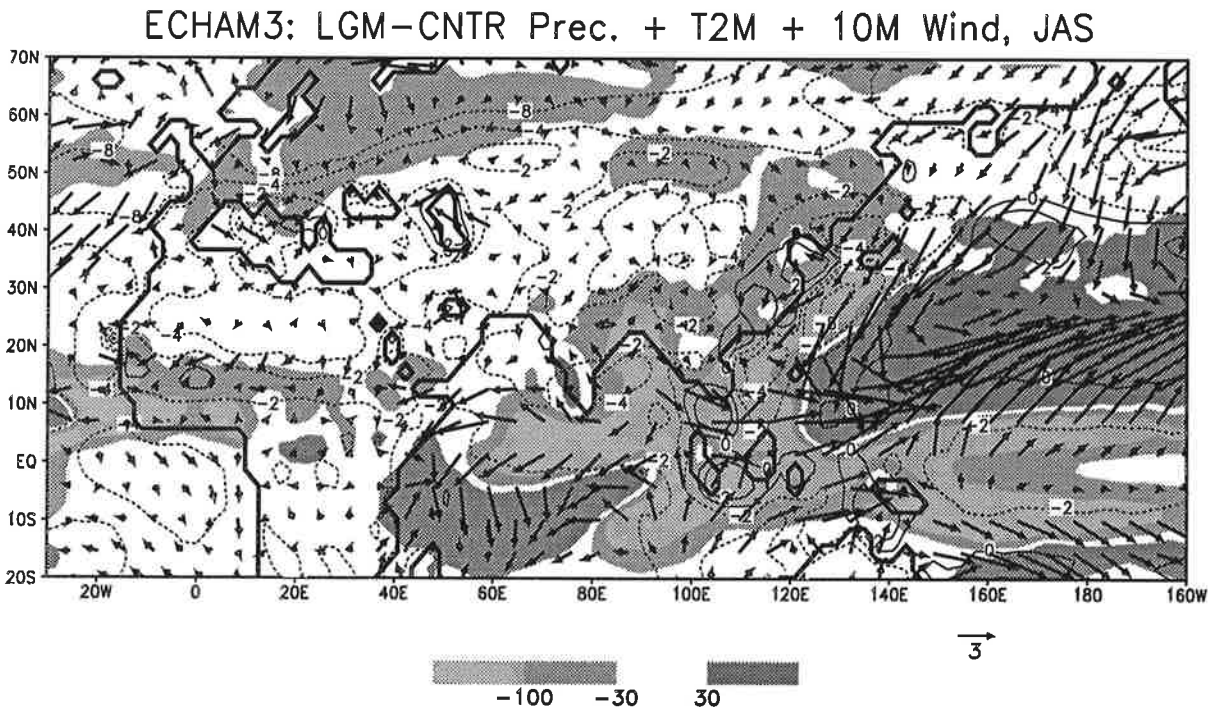


Figure 8: Same as Fig.7 for the winter monsoon (January,February,March).

and the Chinese Sea are directed southeastward against the East Asia monsoon which transports moist air land inwards. A weakened summer monsoon circulation is accompanied by strongly reduced precipitation over eastern India, Southeast Asia, China and Japan (between 50-150mm per month ). The small positive precipitation anomaly in southwestern India is probably an orographic effect. The 120m sea level lowering leads to a relative height increase of the sharp mountains at the western coast of India. In an about 2- 3°C cooler surrounding this may cause a stronger rainout of airmasses which are advected with westerlies from the Arabian Sea.

A wealth of data confirms qualitatively the simulated scenario for the Indian and East Asian summer monsoon. Oceanic dust, pollen and faunal records (Sirocko et al. 1991, Prell and van Campo 1986) in the Arabian Sea are interpreted as indicators for weaker and sligthly southward shifted southwesterlies. Faunal records in the Bay of Bengal(Duplessy 1982) give hints that the freshwater input by river discharge in the northern part of the Bay of Bengal decreased considerably during the last glacial. This indicates less precipitation in northern India and in the Himalayas which are drained by the Ganges and Bramaputra in the Bay of Bengal. Drier conditions prevailed also in China as deduced from lower lake levels (Fang 1991) and loess-paleosol sediments (An et al. 1991). A pollen analysis from marine cores taken off the Pacific coast of Japan yielded a cooler and drier climate than today prevailing in southern Japan (Heusser 1989).

The simulated changes are less unique in winter (Fig.8). The northeasterlies have a stronger eastward component along the Arabian coast and are amplified south of India, over Indochina and in the Chinese Sea. There is no coherent circulation change in the Bay of Bengal and over India. The precipitation anomalies for most of the regions regarded here are rather small during the dry winter season. In fact, a stronger north and northeast component is suggested over the Arabian Sea based on observed larger pollen influx from the Iran steppe (van Campo et al. 1982). Moreover, the reconstructed surface salinity in the Bay of Bengal and South of India is interpreted as an indicator of a stronger northeast winter circulation(Sarkar et al. 1990). Although such a strengthening in this region is not computed by the model we can generally charaterize the simulated climate over India and East Asia for the last glacial as cooler and drier due to a weakened summer monsoon and a partly strengthened northeast winter circulation.

(Kutzbach and Guetter 1986) proposed a mechanism which could explain such changes in the monsoon intensity. The Asian continent gets cooler possibly induced by circulation changes due to the large northern ice sheets and partly due to the $CO_2$ reduction during the LGM. This reduces the Asian heat low in summer and the pressure gradient to the relative cool Indian ocean and the Pacific and intensifies the high pressure system in winter. This cooling could be amplified by the albedo and the hydrological feedback of snow cover anomalies over Siberia and the Tibetan highlands computed in this LGM simulation. On the shorter timescale of interannual variability the influence of such snow cover anomalies on the monsoon intensity has been demonstrated with an older version of the ECHAM (Barnett et al. 1989).

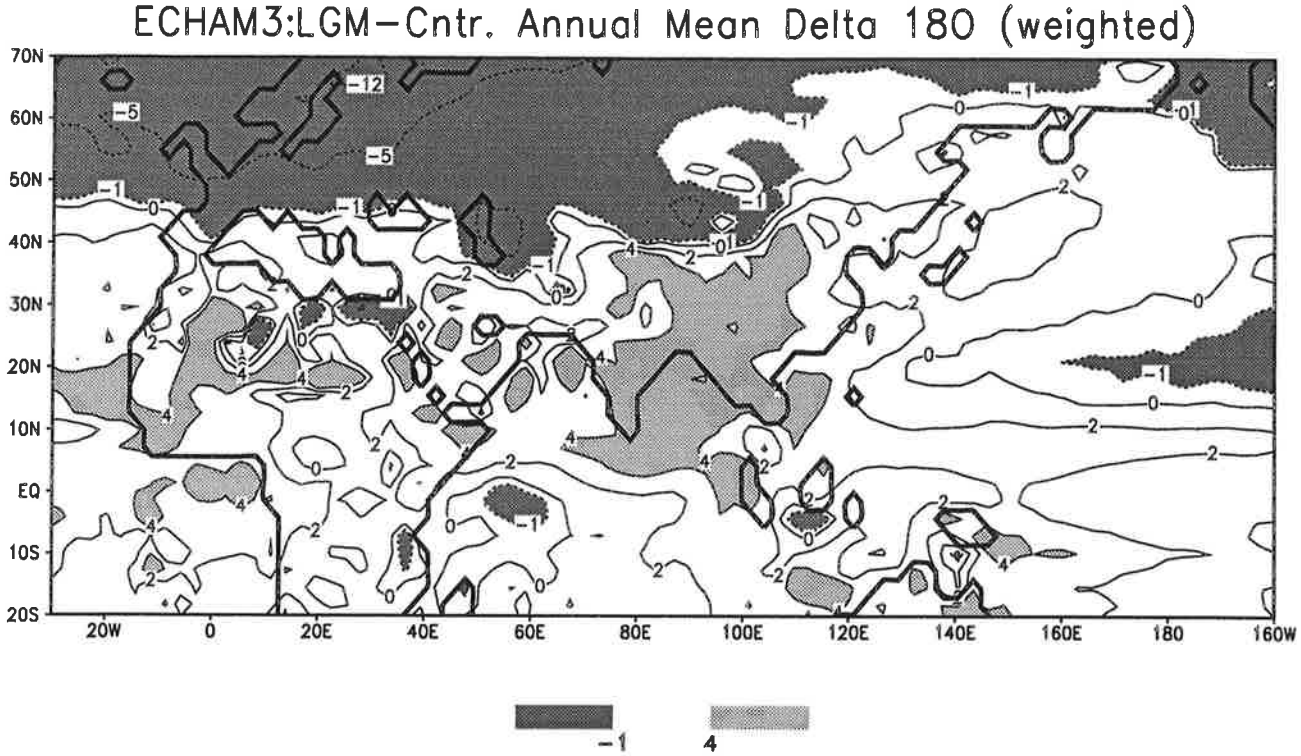


Figure 9: Simulated anomalies (LGM-today) of the annual means of $\delta^{18}O$ in the Asian monsoon area. The isolines are plotted at 4,2,0,-1,-5 ‰. Regions with strong positive anomalies (> 4 ‰) are light shaded and regions with negative anomalies (< -1‰) are dark shaded.

## 4.3 The Isotopic response In the Monsoon Region

What are the regional consequences of the LGM boundary conditions for the isotopic composition of precipitation (Fig.9) ? Obviously the $\delta^{18}O$ anomalies don't follow simply linearly neither the simulated temperature changes nor the precipitation changes (Fig.7+8). Only over Europe north of 45°N $\delta^{18}O$ responds directly to the strong cooling in the vicinity of Fennoscandian ice sheet. The spotty pattern in the northern Sahara is most likely an artefact of simulation problems in arid regions. The only larger negative anomalies in the tropics and subtropics are situated in the subtropical North Pacific and in the western Indian ocean. As mentioned above these regions are wetter than today. Thus the negative $\delta^{18}O$ anomalies follow the amount effect. The strongest positive isotope signal is found in the monsoon area. The positive $\delta^{18}O$ anomalies reach 5‰ over India, the Bay of Bengal and Central China. Apart from the local consequences of weaker monsoon precipitation these anomalies are also caused by circulation changes. The positive gradient from the Chinese Sea to the West of China is produced by the weaker rainout of Pacific air masses near the coast of China (Fig.7) transporting a positive isotope anomaly to the West. Furthermore, the weaker monsoon winds prevent vapour whose source regions are located further away from the coast to be advected into the interior of

the continent. This shortening of the mean distance between the evaporation and the precipitation site also reduces the strength of rainout of a vapour plume and therefore, makes the vapour isotopically heavier. Although the simulated conditions at the precipitation site in western China are about 4°C cooler and only slightly drier (~ 100 mm per year) the $\delta^{18}O$ value is about 4 ‰ higher.

(Fig.10a-c) demonstrates this disagreement between local climate and $\delta^{18}O$ response. The Dunde ice cap is situated on the northern Quinghai Tibetan Plateau (38°N,96°S). The ice cores taken from this glacier reveal a detailed $\delta^{18}O$ record of the last 40,000 years (Thompson et al. 1989). A comparison of the results of the corresponding model grid point (Fig.10b+c) shows clearly that the isotopic composition of precipitation in the seasonal cycle is dominated by the temperature effect under both today (T=0.60 $\delta^{18}O$-12.4, r=0.94) and in the LGM (T=0.52 $\delta^{18}O$-9.1, r=0.90). The temperatures remain below 15°C which is why we would assume that the temperature change of -2.5°C to the LGM produces a corresponding lowering of the $\delta^{18}O$ signal. In contrary we find an about 3 ‰ higher $\delta^{18}O$ value for the LGM simulations. On the other hand, the measured $\delta^{18}O$ change to the LGM in the Dunde ice core is about -2 ‰. It is possible that the model fails to reproduce this $\delta^{18}O$ lowering because of deviations of the model orography from reality. The summit of the Dunde glacier is about 500m higher than the corresponding gridpoint in the GCM. This may influence not only the computed temperature (the annual mean temperature is -7.3 °C (Thompson et al. 1989) instead of -2.0°C in the model) but also the isotopic composition of air masses raining out over the top of the ice cap. Nevertheless, the 3 ‰ higher $\delta^{18}O$ over Dunde demonstrates that the isotopic

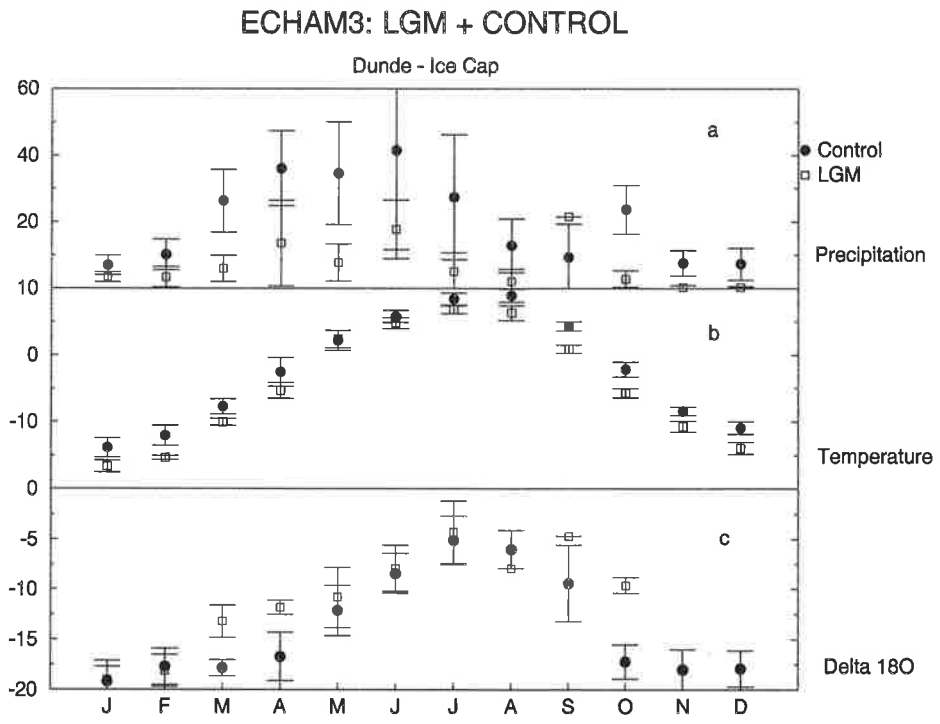


Figure 10: (a) Precipitation (mm/month), (b) surface temperature (°C), and (c) $\delta^{18}O$ for the control run (filled dots) and the LGM run (light squares) at the Dunde ice cap (Quinghai Tibetan plateau ~ 38°N,96°E).

anomalies $\Delta_{LGM-Today}\ \delta^{18}O$ may respond on local temperature changes even with the opposite sign.

On a global scale, the problems of interpreting $\delta^{18}O$ anomalies in terms of temperature changes are made clear by comparing (Fig.11a) with (Fig.3a). The global $\delta^{18}O$- temperature relation remains nearly unchanged under LGM conditions (r=0.96 in the low temperature range Fig.3a). However, the scatter of about 10 % in this relation is amplified if we compare the computed temperature anomalies $\Delta T_{LGM-Today}$ versus the isotopic anomalies $\Delta\ \delta^{18}O_{LGM-Today}$ (Fig.11a). The correlation is only r=0.79 corresponding to an unexplained variance of more than 50% . Even relatively large temperature changes between -5°C and -10°C may be accompanied by positive $\delta^{18}O$ changes. Indeed dramatic temperature changes of more than 10°C are required to get at least qualitatively the "right" isotope response and

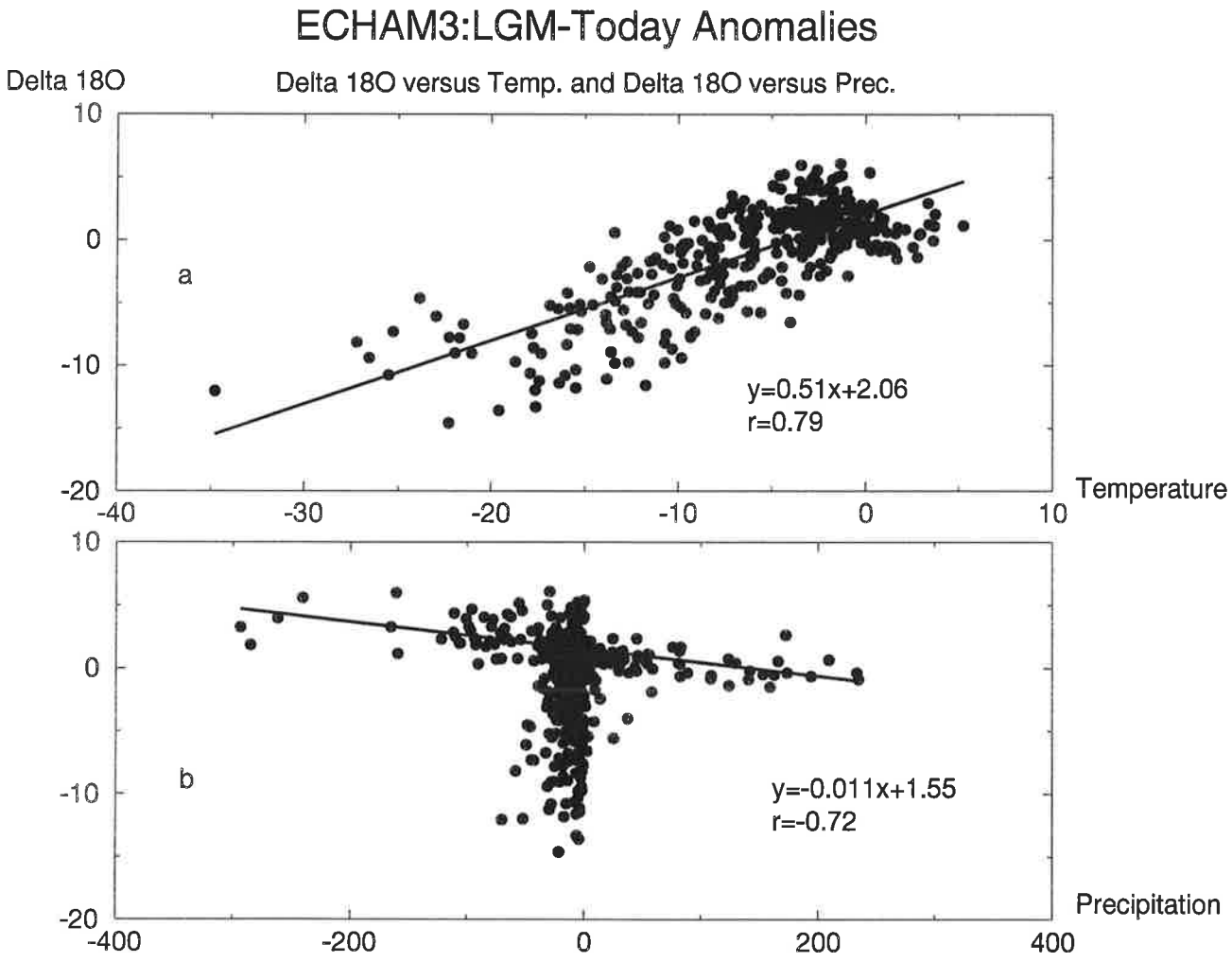


Figure 11: Anomalies (LGM-today) of $\delta^{18}O$ versus anomalies of temperature °C (a) and versus anomalies of precipitation mm per month (b). The results of any 20'th gridpoint are plotted. For the linear regression in (b) all precipitation anomalies below ±30 mm/month are neglected.

to exceed clearly the level of noise in the $\delta^{18}O$- temperature relation.

The scatter of the $\delta^{18}O$- precipitation relation is not that much larger if we consider the anomalies to the LGM (r=-0.72 in Fig.11b compared with r=-0.81 in Fig.4a and r= -0.76 in Fig.4c). If we neglect all points with small precipitation anomalies ( < 30 mm per month) we find a slope of 1.1 ‰ per 100 mm which is roughly in accordance with what we expect from the strength of the present day amount effect (between 1‰ Fig.4a and 2.1‰ Fig.4c per 100 mm).

# 5 Conclusion

We presented here the results of a water isotope model which was embedded into the ECHAM GCM. The model is able to simulate the main features of water isotopes in precipitation under present day conditions on a global scale (temperature, amount, altitude effect etc.) and on a regional scale (monsoon region). Because the description of water isotopes in the model is mainly based on first principles, the successful simulation of the annual mean and the seasonal cycle of the water isotopes constitute an independent test of a GCM's water cycle. Deviations of computed isotopic composition from observations, e.g. the too weak amount effect in the tropics, provide information about weaknesses of the GCM. This will be analyzed in further studies.

How do our results contribute to the discussion about the disturbing influences of the circulation on the $\delta$-temperature or the $\delta$-precipitation relation? (Cole et al. 1993) have shown with a similar isotope model built into the GISS GCM that interannual variability like El Niño or La Niña events produce significant temperature, precipitation and $\delta^{18}O$ anomalies all over the world. Unfortunately, these anomalies are spatially not correlated with each other. (Cole et al. 1993) argue that the circulation pattern causing the temperature anomalies are not identical with the pathways of moisture masses which are responsible for the $\delta^{18}O$ anomalies. These results surely limit the interpretation of high resolution $\delta^{18}O$ records in terms of temperature variations. Under the extremely different boundary conditions of the last glacial not only stronger temperature and $\delta^{18}O$ anomalies than the corresponding interannual anomalies have to be expected but also a different steady state of the circulation. (Charles et al. 1994) investigated the influence of this different steady state on the vapour source distribution of precipitation in Greenland. They found an astonishingly high fraction of North Pacific air masses contributing to the precipitation over the summit of the Greenland ice sheet under LGM conditions. These air masses are strongly depleted because of the long distance to their evaporation site and the corresponding high degree of rainout. Therefore, the snow formed by such air masses would lower the $\delta^{18}O$ measured in the Greenland ice cores without also lowering the paleotemperatures. Nevertheless, these results do not really cast doubt on the interpretation of the measured -7‰ $\delta^{18}O$ change in the Summit ice core in terms of a temperature change. The possible temperature error caused by simulated circulation changes amount at the most 1-2 °C which is rather small compared with the estimated temperature change of about -11 °C between today and the LGM.

This is basically confirmed by our results. The latitudinal gradient of the zonally

averaged $\delta^{18}O$ values of precipitation is tilted under LGM conditions. This means that the $\delta^{18}O$ values following the temperature signal are considerably lower in high latitudes and higher in the tropics and subtropics. But there is a range between 40°N - 40°S where the $\delta^{18}O$ response is not zonally uniform and unique. We investigated the monsoon under LGM conditions and found that the model simulated the monsoon considerably weaker in summer and at least partially intensified in winter. Such a scenario has been shown to be in accordance with a wealth of paleodata. The isotopic composition of precipitation responds to this with a positive $\delta^{18}O$ anomaly over East Asia and India. In particular the computed decoupling of the $\delta^{18}O$ response on LGM condition from the local temperature over the Dunde ice cap demonstrates the importance of long range interactions i.e., the possible shortening of the distance of advected vapour from the evaporation site.

In order to interprete an observed $\delta^{18}O$ change quantitatively in terms of a temperature change, in particular in regions where only a cooling of a few degrees is expected, it seems to be desirable to reconstruct the full pathway of moisture masses to their precipitation site. This was for instance possible in Europe (Rozanski 1985) for the last glacial. The deuterium concentration gradient of precipitation $\delta D$ reconstructed from the western coast of Europe to the East allowed an interpretation as indicator of a temperature shift of about -7°C. These results were in agreement with our simulations (not shown here) (Hoffmann 1995).

The model failed to reproduce the observed $\delta^{18}O$ lowering of -2 ‰ in the Dunde ice core. Further studies have to clarify if this is a result of the model resolution or of other factors. Colder tropical SST's than the CLIMAP temperatures for instance have been suggested because much lower snow lines for the LGM than today are observed in the tropics. Such a lowering is not in accordance with GCM results forced with CLIMAP SST's (Rind and Peteet 1985). Possible cooler temperatures would of course affect the isotopic composition of vapour and the entire monsoon circulation as well. In any case, more data of $\delta^{18}O$ in paleoprecipitation covering a more extended area are needed in order to evaluate regionally both the computed response of the water isotope model and the interpretation of $\delta^{18}O$ records.

# References


An, Z., Kukla, G., Porter, S. and Jo, X. (1991), 'Magnetic suszeptibility evidence of monsoon variation on the loess plateau of central China during the last 130,000 years', *Quat.Res.* **36**, 29–36.

Barnett, T., Dümenil, L., Schlese, U. and Latif, M. (1989), 'The effect of Eurasian snow cover on regional and global climate variations', *Journal of Atmospheric Sciences* **46**, 661–685.

Becker, B., Kromer, B. and Trimborn, P. (1991), 'A stable-isotope tree ring timescale of the late glacial/holocene boundary', *Nature* **353**, 647–649.

Berger, A. (1978), 'Long-term variations of daily insolation and quaternary climatic changes', *Journ. of Atmos.Sci.* **35**, 2362–2367.

Bradley, R. (1985), *Quaternary Paleoclimatology: Methods of Paleoclimatic Reconstruction*, Allen and Unwin. Boston,Mass.

Charles, C., Rind, D., Jouzel, J., Koster, R. and Fairbanks, R. (1994), 'Glacial-Interglacial changes in moisture sources for Greenland: influence on the ice core record of climate', *Science* **263**, 508–511.

CLIMAP:81 (1981), 'Climate:Long-range investigation, mapping and prediction (CLIMAP) project members, seasonal reconstruction of the earth's surface at the last glacial maximum', Map.Chart.Ser., MC-36, Geol.Soc.of Am., Boulder.

Cole, J. and Fairbanks, R. (1990), 'The southern oscillation recorded on the oxygen isotopes of corals from Taraw atoll', *Paleoceanography* **5**, 669–683.

Cole, J., Rind, D. and Fairbanks, R. (1993), 'Isotopic responses to interannual variability simulated by an AGCM', *Quat.Sci.Rev.* **12**, 387–406.

Covich, A. and Stuiver, M. (1974), 'Changes in oxygen 18 as a measure of long-term fluctuations in tropical lake levels and mooluscan populations', *Limnology and Oceanography* pp. 682–691.

Dansgaard, W. (1964), 'Stable isotopes in precipitation', *Tellus* **16**, 436–468.

Duplessy, J. (1982), 'Glacial to interglacial contrasts in the northern Indian Ocean', *Nature* **295**, 494–498.

Duplessy, J., Moyes, J. and Pajol, C. (1980), 'Deep water formation in the North Atlantic ocean during the last ice age', *Nature* **286**, 479–482.

Eicher, U. and Siegenthaler, U. (1976), 'Palynological and oxygen isotope investigations on late- glacial sediment cores from Swiss lakes', *Boreas* **5**, 109–117.

Fairbanks, R. and Matthews, R. (1978), 'The marine oxygen isotope record in pleistocene coral, Barbados, WestIndies', *Quat.Res.* **10**, 181–196.

Fang, J. (1991), 'Lake evolution during the past 30,000 years in China and its implications for environmental change', *Quat.Res.* **36**, 37–60.

Gasse, F., Arnold, M., Fontes, J., Fort, M., Gibert, E., Huc, A., Li, B., Liu, Q., Melieres, F., van Campo, E., Wang, F. and Zhan, Q. (1991), 'A 13000 year climate record from western Tibet', *Nature* **353**, 742–745.

Goodfriend, G. (1991), 'Holocene trends in 18O in land snail shells from the Negev desert and their implications for changes in rainfall source areas', *Quat.Res.* **35**, 417–426.

Grootes, P., Stuiver, M., Thompson, L. and Mosley-Thompson, L. (1989), 'Oxygen isotope changes in tropical ice, Quelcaya, Peru', *Journal of Geophys.Res.* **94**, 1187–1194.

Harmon, R. and Schwarz, H. (1981), 'Changes of $^{2}H$ and $^{18}O$ enrichment of meteoric water and pleistocene glaciation', *Nature* **290**, 125–128.

Harmon, R., Schwarz, H. and O'Neill, J. (1981), 'D/H ratios in speleothem fluid inclusions. A guide to variations in the isotopic composition of meteoric precipitation?', *Earth Planet.Sci.Lett.* **42**, 254–266.

Heusser, L. (1989), Northeast Asian climatic change over the last 140,00 years inferred from pollen in marine cores taken off the pacific coast of Japan, *in* 'Paleoclimatology and paleometeorology: modern and past pattern of global atmospheric transport', Leinen M. and Sarntheim M., pp. 665–692.

Hoffmann, G. (1995), Wasserisotope im allgemeinen Zirkulationsmodell ECHAM, PhD thesis, Universität Hamburg.

Hoffmann, G. and Heimann, M. (1993), Water tracers in the ECHAM GCM, *in* 'Isotope techniques in the study of the past and current environmental changes in the hydrosphere and the atmosphere', I.A.E.A.

IAEA (1992), Statistical Treatment of Data on environmental isotopes in precipitation, Technical report, I.A.E.A.

Johnsen, S., Clausen, H., Dansgaard, W. and Fuhrer, N. (1992), 'Irregular glacial interstadials recorded in a new Greenland ice core', *Nature* **359**, 311–313.

Joussaume, J., Sadourny, R. and Jouzel, J. (1984), 'A general circulation model of water isotope cycles in the atmosphere', *Nature* **311**, 24–29.

Jouzel, J. and Merlivat, L. (1984), 'Deuterium and Oxygen 18 in Precipitation, Modelling of the isotopic effects during snow formation', *Journal of Geophys.Res.* **89**, 11749–11757.

Jouzel, J., Russell, G., Suozzo, R., Koster, R., White, J. and Broecker, W. (1987), 'Simulations of the HDO and $^{1}H_{2}\,^{18}O$ atmospheric cycles using the NASA GISS General Circulation Model: The seasonal cycle for present day conditions', *Journal of Geophys.Res.* **92**, 14739–14760.

Kutzbach, J. and Guetter, P. (1986), 'The influence of changing orbital parameters and surface boundary conditions on climate simulations for the past 180,000 years', *Journal of Atmospheric Sciences* **43**(16), 1726–1759.

Lautenschlager, M. and Herterich, K. (1990), 'Atmospheric response to ice age conditions: Climatology near the earth surface', *J.Geophys.Res.* **95**(D13), 11547–22557.

Lipp, J., Trimborn, P., Fritz, P., Moser, H., Becker, B. and Frenzel, B. (1991), 'Stable isotopes in tree ring cellulose and climatic change', *Tellus* **43B**, 322–330.

Lorius, C. (1983), Antarctica: Survey of near–surface mean isotopic values, *in* G. de Q. Robin, ed., 'The climate record of the polar ice sheet', Cambridge University Press, New York, pp. 52–56.

Lorius, C., Jouzel, J., Ritz, C., Merlivat, L., Barkov, N., Korotkevich, Y. and Kotlyakov, V. (1985), 'A 150.000 year climatic record from Antarctic ice', *Nature* **316**, 591–596.

Majoube, M. (1971), 'Fractionnement en oxygen 18 et en deuterium entre l'eau et sa vapeur', *J.Chim.Phys.* **10**, 1423–1436.

Merlivat, L. and Jouzel, J. (1979), 'Global climatic interpretation of the deuterium–oxygen 18 relationship for precipitation', *Journal of Geophys. Res.* **84**, 5029–5033.

Modellbetreuungsgruppe (1992), The ECHAM3 atmospheric general circulation model, Technical Report 6, Deutsches Klimarechenzentrum, Bundesstr. 55 D-20146 Hamburg.

Prell, W. and Kutzbach, J. (1987), 'Monsoon variability over the apst 150,000 years', *Journal of Geophys. Res.* **92**(D7), 8411–8425.

Prell, W. and van Campo, E. (1986), 'Coherent response of Arabian Sea upwelling and pollen transport to late quaternary monsoonal winds', *Nature* **323**, 526–528.

Rind, D. (1987), 'Components of Ice-Age-Circulation', *Journal of Geophys. Res.* **92**, 4241–4281.

Rind, D. and Peteet, D. (1985), 'Terrestrial conditions at the last glacial maximum and CLIMAP sea-surface temperature: Are they consistent?', *Quat.Res.* **24**, 1–22.

Rozanski, K. (1985), 'Deuterium and 18O in European groundwater - links to atmospheric circulation in the past', *Chem.Geol.* **52**, 349–363.

Rozanski, K., Sonntag, C. and Münnich, K. (1982), 'Factors controlling stable isotope composition of european precipitation', *Tellus* **34**, 142–150.

Salati, E., Dall'Olio, A., Matsui, E. and Gat, J. (1979), 'Recycling of water in the Amazone Basin: an isotopic study', *Water Resour.Res.* **15**, 1250–1257.

Sarkar, A., Ramesh, R., Bhattacharga, S. and Rajagopalan, G. (1990), 'Oxygen isotope evidence for a stronger winter monsoon current during the last glaciation', *Nature* **343**, 549–551.

Sirocko, F., Sarntheim, M., Lange, H. and Erlenkeuser, H. (1991), 'Atmospheric summer circulation and coastal upwelling in the arabian sea during the holocene and the last glaciation', *Quat.Res.* **36**, 72–93.

Sonntag, C., Klitzsch, E., Löhert, P., El-Shazly, E., Münnich, K., Junghans, C., Thorweike, U., Weistroffer, K. and Swailem, F. (1978), Paleoclimatic information from deuterium and oxygen-18 in carbon 14 dated north Saharian groundwater, *in* 'Isotope hydrology II', I.A.E.A., pp. 569–581.

Stewart, M. (1975), 'Stable isotope fractionation due to evaporation and isotopic exchange of falling waterdrops: applications to atmospheric processes and evaporation of lakes', *Journal of Geophys.Res.* **80**, 1133–1146.

Street-Perrot, F. and Harrison, S. (1985), Lake levels and climate reconstruction, *in* 'Paleoclimate analysis and modeling', Hecht A.D., pp. 291–340.

Stuiver, M. (1970), 'Oxygen and carbon isotope ratios of fresh water carbonates as climatic indicators', *Journal of Geophys.Res.* **75**, 5247–5257.

Taylor, C. (1972), The vertical variations of isotopic concentrations of tropospheric water vapour over continental Europe and their relationship to tropospheric structure, Technical Report INS-R-107, Inst.Nuclear Sciences,Lower Hutt,NewZealand.

Thompson, L., Mosley-Thompson, L., Davis, M., Bolzan, J., Dai, J., Yao, T., Gundestrup, N., Wu, X., Klein, L. and Xie, Z. (1989), 'Holocene-late pleistocen climatic ice core records from Quinghai-Tebetan Plateau', *Science* **246**, 474–477.

Tushingham, A. and Peltier, W. (1991), 'ICE-3G: a new global model of late pleistocene deglaciation based upon geophysical predictions pf past-glacial relative sea-level change', *Journ. of Geophys.Res.* **96**, 4497–4523.

van Campo, E., Duplessy, J. and Rossignol-Strick, M. (1982), 'Climatic conditions deduced from a 150 kyr oygen isotope- pollen record from the Arabian Sea', *Nature* **296**, 56–59.

White, J. (1989), Stable hydrogen isotope retios in plants: a review of current theory and some potential applications, *in* 'Stable isotopes in ecological research', Springer Verlag New York, pp. 142–162.

WMO (1993), Report of ninth session of the CAS/JSC working group on numerical experimentation, *in* 'WMO atmospheric research and environmental programme', WMO.

Yapp, C. and Epstein, S. (1977), 'Climatic implications of D/H ratios of meteoric water over North America (9500–22000BP) as inferred from ancient wood cellulose C-H hydrogen', *Earth Planet.Sci.Lett.* **34**, 330–350.

Zimmerman, U., Ehhalt, D. and Münnich, K. (1967), Soil water movement and evapotranspiration change in the isotopic composition of the water, *in* 'Isotopes in hydrology', pp. 567–585.